Mathematical Modelling and Control

https://www.aimspress.com/journal/mmc

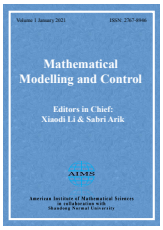

MMC, 4(3): 316–335.
DOI: 10.3934/mmc.2024026
Received: 28 December 2022
Revised: 13 May 2023
Accepted: 20 June 2023
Published: 09 September 2024

Research article

Modeling and optimal control of COVID-19 and malaria co-infection based on vaccination

Yaxin Ren[1] **and Yakui Xue**[2,*]

[1] Laiwu Technician Institute, Ji'nan 271100, China

[2] School of Mathematics, North University of China, Taiyuan 030051, China

* **Correspondence:** Email: xyk5152@163.com.

Abstract: Malaria is a serious health problem in Africa, and the ongoing COVID-19 pandemic has affected the implementation of key malaria control interventions. This jeopardizes the gains made in malaria. As a result, a new co-infection model of COVID-19 and malaria is constructed, and the role of vaccination in COVID-19-malaria co-infection is analyzed. The existence and stability of the equilibria of each single infection are first studied by their respective basic reproduction numbers. When the basic reproduction numbers R_{C0} and R_{M0} are both below unity, the COVID-19-malaria-free equilibrium is locally asymptotically stable. Sensitivity analysis reveals that the main parameters affecting the spread of diseases are their respective disease transmission rate and vaccine efficacy. Further, we introduce the effect of vaccination rate and efficacy on controlling the co-infected population. It also shows that under the condition of a low recovery rate caused by the shortage of medical resources, improving the vaccination rate and effectiveness of vaccines has a positive impact on suppressing diseases. The model is then extended into an optimal control system by introducing prevention and treatment measures for COVID-19 and malaria. The results suggest that applying each strategy alone can reduce the scale of co-infection, but strategy A increases the number of malaria cases and strategy B prolongs the period of COVID-19 infection. Measures to control COVID-19 must be combined with efforts to ensure malaria control is maintained.

Keywords: COVID-19; malaria; co-infection; vaccination; optimum control

1. Introduction

Malaria is a vector-borne infection caused by the bite of a mosquito carrying the plasmodium parasite. Of all infectious diseases, malaria remains one of the largest contributors to the global burden and continues to receive worldwide attention in terms of suffering and death (see [1]). Efforts have been made to curb malaria transmission (see the works [1, 2]), for example, through the use of effective antimalarial drugs [3] and infecting the mosquito population with Wolbachia [4]. Also, COVID-19 was caused by the outbreak of SARS-CoV-2 at the end of 2019, which spreads rapidly around the world and poses an unprecedented challenge to global health. The clinical manifestations of COVID-19 include fever, difficulty breathing, dry cough, and a range of symptoms that overlap those of malaria [5]. This makes diagnosis and treatment challenging. In addition, malaria cases are mainly distributed in African countries, which have a heavy burden of infectious diseases and weak public health infrastructure. At the same time, most of these countries have limited health budgets [6], and controlling the spread of COVID-19 will have an impact on the intervention level of other infectious diseases [7]. This provides a geographical advantage for co-infection of COVID-19 and malaria. Hence, Gutman et al. [8] pointed out that co-infection of malaria and COVID-19 can occur in those countries where malaria is endemic. Many scientists also believed COVID-19 would hit Africa hard [9–11]. Moreover, there are also concerns about the broader health, economic, and social impacts of measures to mitigate the spread of COVID-19, not just about the disease itself. From the aforementioned reasons, co-infection is a concern, and it

is important to theoretically investigate the impact of control measures on their long-term dynamics.

Mathematical models are important tools for predicting and simulating the spread of epidemics, and can provide timely information for decision-making [12–15]. At the beginning of the COVID-19 outbreak, a large number of papers about COVID-19 infection modeling have been produced. Scholars have made many contributions to COVID-19 research from the perspective of micro [16, 17], macro (see [18, 19]), or using fractional order models (see, for example, [19–21]). However, reports of co-infection of COVID-19 and malaria are rare, and the researchers are focused on studying the complex dynamics and possible control of this global infection. Tchoumi et al. [13] constructed a mathematical model incorporating some epidemiological features of the co-dynamics of both malaria and COVID-19. They showed that applying both COVID-19 and malaria protective strategies could help reduce their spread in comparison to applying each preventive measure singly, but only control strategies for non-pharmaceutical interventions were analyzed. Ojo et al. analyzed the impact of COVID-19 on a malaria-dominated region and investigated the impact of threshold and co-infection transmission rate on the synergistic relationship between the two diseases [14]. The co-infection of two diseases can have devastating consequences globally, so research on the co-infection of COVID-19 and other diseases is booming. For example, COVID-19 and dengue [22], COVID-19 and HIV [23, 24], COVID-19 and cholera [25] and other co-infections [26–30].

Some researchers developed dynamic models of epidemiology for infectious disease based on preventive measures (social distancing, wearing masks, and lockdown) [21, 31, 32]. Couras et al. [33] introduced two control functions in the SEIR model representing vaccination and plasma transfusion, and the results showed that the strategies may have a real application for the COVID-19 pandemic. So, among the measures to control the spread of disease, vaccination is an effective way to cut the chain of transmission, prevent, and reduce virus infection [34]. There are also some studies on the impact of vaccination on the spread of COVID-19. For example, see [15, 18, 35–37] and the references therein. Despite these control measures, controlling the spread of COVID-19 remains a challenge due to inadequate vaccine supply, vaccine uptake hesitancy, vaccine efficacy, vaccine waning, non-adherence to public health orders, and virus mutation [38].

In addition to vaccination, asymptomatic carriers also play an important role in infectious disease modeling [39], neither of which has been mentioned in literature [13]. Currently, there are insufficient studies to analyze the impact of vaccination on co-infection with COVID-19 and malaria. To fill this gap, we consider and improve the limitations in [13] in modeling and formulate a COVID-19 and malaria co-infection model to study the effects of basic reproduction numbers and vaccination on the COVID-19-malaria co-infection. This study is seemingly the first of its kind to theoretically detailly investigate the effects of vaccination on the co-dynamics of COVID-19 and malaria, as well as the key prevention and therapeutic measures that are incorporated into the control system. Then, we discuss numerical simulation depicts results.

The structure of this paper is as follows: In Section 2, the co-infection model of malaria and COVID-19 is established. In Section 3, the sub-models are first analyzed, and then the co-infection model is studied. To mitigate the spread of these two diseases, four control measures are incorporated into the co-infection model, and the optimal control problem is explored in Section 4. In Section 5, numerical simulations are carried out. This includes data fitting, sensitivity analysis, stability analysis, the impact of vaccination parameters on disease transmission and control, and the implementation of control strategies. Section 6 is the summary part.

2. Model formulation

The human population at time t, denoted by $N(t)$, is divided into susceptible individuals $S(t)$, individuals vaccinated against COVID-19 $V(t)$, asymptomatic infectious individuals $A(t)$, symptomatic infectious individuals $I(t)$, individuals infected with malaria $E(t)$, individuals infected with both malaria and COVID-19 $I_E(t)$, and recovered individuals $R(t)$. So that,

$$N(t) = S(t) + V(t) + A(t) + I(t) + E(t) + I_E(t) + R(t).$$

The mosquito population at time t, denoted by $N_v(t)$, is divided into susceptible mosquitoes $S_v(t)$, mosquitoes exposed to the malaria parasite $E_v(t)$, and infectious mosquitoes $I_v(t)$. So that,

$$N_v(t) = S_v(t) + E_v(t) + I_v(t).$$

The model has the following assumptions:

(i) Co-infected individuals can not transmit the mixed infections at the same time;

(ii) Co-infected individuals can recover either from COVID-19 or malaria but not from the mixed infection at the same time.

The changes that occur in each compartment in disease transmission can be interpreted by Figures 1 and 2.

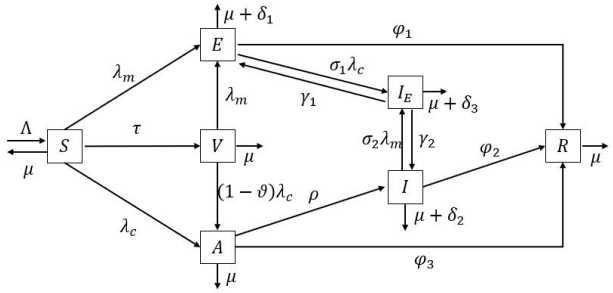

Figure 1. Transmission diagram of the human component of the model.

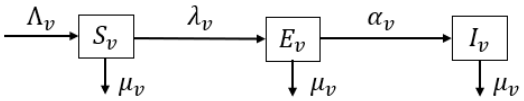

Figure 2. Transmission diagram of the mosquito component of the model.

The system of differential equations related to the transmission diagram Figures 1 and 2 is as follows:

$$\begin{cases} \dfrac{dS(t)}{dt} = \Lambda - (\lambda_m + \lambda_c + \tau) S - \mu S, \\ \dfrac{dV(t)}{dt} = \tau S - ((1-\theta)\lambda_c + \lambda_m) V - \mu V, \\ \dfrac{dA(t)}{dt} = \lambda_c (S + (1-\theta) V) - (\rho + \varphi_3 + \mu) A, \\ \dfrac{dI(t)}{dt} = \rho A - \sigma_2 \lambda_m I - (\delta_2 + \varphi_2 + \mu) I + \gamma_2 I_E, \\ \dfrac{dE(t)}{dt} = \lambda_m (S + V) - \sigma_1 \lambda_c E - (\delta_1 + \varphi_1 + \mu) E + \gamma_1 I_E, \\ \dfrac{dI_E(t)}{dt} = \sigma_1 \lambda_c E + \sigma_2 \lambda_m I - (\delta_3 + \mu) I_E - (\gamma_1 + \gamma_2) I_E, \\ \dfrac{dR(t)}{dt} = \varphi_1 E + \varphi_2 I + \varphi_3 A - \mu R, \\ \dfrac{dS_v(t)}{dt} = \Lambda_v - \lambda_v S_v - \mu_v S_v, \\ \dfrac{dE_v(t)}{dt} = \lambda_v S_v - (\alpha_v + \mu_v) E_v, \\ \dfrac{dI_v(t)}{dt} = \alpha_v E_v - \mu_v I_v, \end{cases} \tag{2.1}$$

where,

$$\lambda_c = \frac{\beta_c (\varepsilon_1 A + I + I_E)}{N},$$

$$\lambda_m = \frac{\beta_m b I_v}{N}$$

and

$$\lambda_v = \frac{\beta_v b (E + I_E)}{N}.$$

All variables and parameters of model (2.1) are non-negative at time

$$t \geq 0.$$

In this paper, as in article [13], the incidence of the disease is considered as the standard incidence type. The descriptions and values of other associated parameters are provided in Tables 1 and 2.

Table 1. Parameters description.

Parameter	Description
Λ	Recruitment rate of humans
Λ_v	Recruitment rate of mosquitoes
β_c	Contact rate for COVID-19 transmission
β_m	Malaria transmission probability per mosquito bite
β_v	Transmission probability in vectors from infected humans
φ_1	Malaria recovery rate for singly-infected
φ_2	Recovery rate of symptomatic infectious individuals
φ_3	Recovery rate of asymptomatic infectious individuals
τ	COVID-19 vaccination rate
δ_1	Malaria induced death rate
δ_2	COVID-19 induced death rate
δ_3	Disease induced death rate for individuals in compartment I_E
μ	Mortality rate of humans
μ_v	Natural mortality rate of mosquitoes
ε_1	Modification factor concerning transmission from compartment A
b	Number of bites per day by female mosquitoes
θ	COVID-19 vaccine efficacy
ρ	Rate of onset of symptoms
γ_1	Rate at which co-infected individuals (I_E) recover from COVID-19-only
γ_2	Rate at which co-infected individuals (I_E) recover from malaria-only
σ_1	Factor that enhances acquiring of COVID-19 infection after being infected with malaria
σ_2	Factor that enhances the acquisition of malaria infection after being infected with COVID-19
α_v	Progression rate from exposed to infectious class

Table 2. Parameters used in the model.

Parameter	Value	Reference
Λ	$\frac{39609704}{64.13\times365}$	[24]
Λ_v	$\frac{5000}{21}$	[40]
β_c	0.4531	[13]
β_m	0.5	[13]
β_v	0.52	Assumed
φ_1	0.038	[28]
φ_2	0.022	Assumed
φ_3	0.05	Assumed
τ	0.02	[37]
δ_1	0.0019	[28]
δ_2	0.015	[29]
δ_3	0.4	Assumed
μ	$\frac{1}{64.13\times365}$	[24]
μ_v	0.033	[4]
ε_1	0.45	[15]
b	4.3×0.33	[13]
θ	0.8	[15]
ρ	0.07	[30]
γ_1	0.055	Assumed
γ_2	0.038	Assumed
σ_1	1.02	[13]
σ_2	1.01	[13]
α_v	0.1	[13]

3. Model analysis

Before analyzing the dynamics of the full model, analyze the sub-models first, i.e., COVID-19-only model and malaria-only model.

3.1. COVID-19-only model

The COVID-19-only sub-model is not related to malaria, so the COVID-19-only model is obtained by setting

$$E(t) = I_E(t) = S_v(t) = E_v(t) = I_v(t) = 0$$

in (2.1). We have

$$\begin{cases} \dfrac{dS(t)}{dt} = \Lambda - (\lambda_c + \tau) S - \mu S, \\ \dfrac{dV(t)}{dt} = \tau S - (1-\theta)\lambda_c V - \mu V, \\ \dfrac{dA(t)}{dt} = \lambda_c (S + (1-\theta) V) - (\rho + \varphi_3 + \mu) A, \\ \dfrac{dI(t)}{dt} = \rho A - (\delta_2 + \varphi_2 + \mu) I, \\ \dfrac{dR(t)}{dt} = \varphi_2 I + \varphi_3 A - \mu R, \end{cases} \tag{3.1}$$

where

$$\lambda_c = \frac{\beta_c (\varepsilon_1 A + I)}{N}$$

is the force of infection and

$$N(t) = S(t) + V(t) + A(t) + I(t) + R(t).$$

By adding up all the equations of the model (3.1), the total human population is given by

$$\frac{\mathrm{d}N(t)}{\mathrm{d}t} = \Lambda - \mu N - \delta_2 I. \tag{3.2}$$

Solving the differential Eq (3.2), we have

$$N(t) \leq N(0)\, e^{-\mu t} + \frac{\Lambda}{\mu}\left(1 - e^{-\mu t}\right). \tag{3.3}$$

Thereby, $0 \leq N(t) \leq \frac{\Lambda}{\mu}$ as $t \to +\infty$. In the region

$$\Gamma_C = \left\{(S, V, A, I, R) \in R_+^5 : N(t) \leq \frac{\Lambda}{\mu}\right\},$$

all solutions of the model (3.1) starting in Γ_C remain in Γ_C for all $t \geq 0$. Thus, we will consider the dynamics of model (3.1) in Γ_C.

3.1.1. Stability of the disease-free equilibrium

The disease-free equilibrium of model (3.1) is given by

$$E_{C0} = \left(\frac{\Lambda}{\mu+\tau}, \frac{\Lambda\tau}{\mu(\mu+\tau)}, 0, 0, 0\right). \tag{3.4}$$

According to the next generation matrix method [41], the matrices F and V are calculated by

$$\mathcal{F} = \begin{pmatrix} \lambda_c (S + (1-\theta) V) \\ 0 \end{pmatrix}$$

and

$$\mathcal{V} = \begin{pmatrix} (\rho + \varphi_3 + \mu) A \\ (\delta_2 + \varphi_2 + \mu) I - \rho A \end{pmatrix}.$$

Then,

$$F = \begin{pmatrix} \frac{\beta_c \varepsilon_1 [\mu + \tau(1-\theta)]}{\mu+\tau} & \frac{\beta_c [\mu + \tau(1-\theta)]}{\mu+\tau} \\ 0 & 0 \end{pmatrix}$$

and

$$V = \begin{pmatrix} \rho + \varphi_3 + \mu & 0 \\ -\rho & \delta_2 + \varphi_2 + \mu \end{pmatrix}.$$

Thus, R_{C0} is given by

$$R_{C0} = \frac{\beta_c \left[(\delta_2 + \varphi_2 + \mu)\varepsilon_1 + \rho\right][\mu + (1-\theta)\tau]}{(\rho + \varphi_3 + \mu)(\delta_2 + \varphi_2 + \mu)(\mu + \tau)}. \tag{3.5}$$

From Theorem 2 of [41], the result follows:

Lemma 3.1. *The disease-free equilibrium E_{C0} of the COVID-19-only model* (3.1) *is locally asymptotically stable if $R_{C0} < 1$, and unstable if $R_{C0} > 1$.*

Theorem 3.1. *The disease-free equilibrium E_{C0} of the COVID-19-only model* (3.1) *is globally asymptotically stable if $R_{C0} < 1$.*

Proof. Consider a Lyapunov function $L_1(t)$ as follows

$$L_1 = (\delta_2 + \varphi_2 + \mu) A + \frac{\beta_c [\mu + (1-\theta)\tau]}{\mu + \tau} I. \tag{3.6}$$

From model (3.1), as

$$\begin{aligned} t \to \infty, N \to N_\infty &= S_\infty + V_\infty + A_\infty + I_\infty + R_\infty \\ &\geq S_\infty + V_\infty \\ &= S_0 + V_0. \end{aligned}$$

Since $S \leq S_0$ and $V \leq V_0$, the following inequalities which will be used subsequently hold:

$$\frac{S}{N} \leq \frac{S_0}{S_0 + V_0}$$

and

$$\frac{V}{N} \leq \frac{V_0}{S_0 + V_0}.$$

Thus,

$$\begin{aligned} \dot{L}_1 =& (\delta_2 + \varphi_2 + \mu)\left[\lambda_c (S + (1-\theta) V) - (\rho + \varphi_3 + \mu) A\right] \\ &+ \frac{\beta_c [\mu + (1-\theta)\tau]}{\mu + \tau}\left[\rho A - (\delta_2 + \varphi_2 + \mu) I\right] \\ \leq& \frac{\beta_c (\delta_2 + \varphi_2 + \mu)[\mu + (1-\theta)\tau]}{\mu + \tau}(\varepsilon_1 A + I) \\ &- (\delta_2 + \varphi_2 + \mu)(\rho + \varphi_3 + \mu) A + \frac{\beta_c \rho [\mu + (1-\theta)\tau]}{\mu + \tau} A \\ &- \frac{\beta_c (\delta_2 + \varphi_2 + \mu)[\mu + (1-\theta)\tau]}{\mu + \tau} I \\ =& \frac{\beta_c (\delta_2 + \varphi_2 + \mu)[\mu + (1-\theta)\tau]}{\mu + \tau}\left(\varepsilon_1 + \frac{\rho}{\delta_2 + \varphi_2 + \mu}\right) A \\ &- (\delta_2 + \varphi_2 + \mu)(\rho + \varphi_3 + \mu) A \\ =& (\delta_2 + \varphi_2 + \mu)(\rho + \varphi_3 + \mu)(R_{C0} - 1) A. \end{aligned} \tag{3.7}$$

It can be verified that $\dot{L}_1 \leq 0$ for $R_{C0} < 1$. Thus, by LaSalle's invariance principle [42], the disease-free equilibrium E_{C0} of model (3.1) is global asymptotically stable when $R_{C0} < 1$. □

3.1.2. Existence and stability of the endemic equilibrium

Solving the COVID-19-only sub-model (3.1) at an arbitrary equilibrium denoted by

$$E_{C1} = (S^*, V^*, A^*, I^*, R^*)$$

yields

$$E_{C1} = \left(\frac{\Lambda}{\mu+\tau+\lambda_c^*}, \frac{\tau S^*}{\mu + (1-\theta)\lambda_c^*}, \frac{\lambda_c^* [S^* + (1-\theta) V^*]}{\rho + \varphi_3 + \mu}, \frac{\rho A^*}{\delta_2 + \varphi_2 + \mu}, \frac{\varphi_2 I^* + \varphi_3 A^*}{\mu} \right), \tag{3.8}$$

where

$$\lambda_c^* = \frac{\beta_c (\varepsilon_1 A^* + I^*)}{S^* + V^* + V^* + I^* + R^*}. \tag{3.9}$$

Note that

$$\varepsilon_1 A^* + I^* = \frac{\Lambda \lambda_c^* [\mu + (1-\theta)(\lambda_c^* + \tau)]}{(\rho + \varphi_3 + \mu)(\mu+\tau+\lambda_c^*)[\mu + (1-\theta)\lambda_c^*]} \left(\varepsilon_1 + \frac{\rho}{\delta_2 + \varphi_2 + \mu} \right). \tag{3.10}$$

From Eq (3.9), we obtain

$$\varepsilon_1 A^* + I^* = \frac{\lambda_c^* N^*}{\beta_c} \tag{3.11}$$

From Eqs (3.10) and (3.11) and after some little rearrangements, we obtain the following polynomial

$$a_0 \lambda_c^{*2} + a_1 \lambda_c^* + a_2 = 0 \tag{3.12}$$

and

$$\begin{aligned} a_0 &= (\rho + \varphi_3 + \mu)(\delta_2 + \varphi_2 + \mu) N^* (1-\theta), \\ a_1 &= \mu(\rho + \varphi_3 + \mu)(\delta_2 + \varphi_2 + \mu) N^* \\ &\quad + (\rho + \varphi_3 + \mu)(\delta_2 + \varphi_2 + \mu) N^* (\mu+\tau)(1-\theta) \\ &\quad - \Lambda \beta_c (1-\theta)[\varepsilon_1 (\delta_2 + \varphi_2 + \mu) + \rho], \\ a_2 &= (\rho + \varphi_3 + \mu)(\delta_2 + \varphi_2 + \mu) \Lambda (\mu+\tau)(1 - R_{C0}). \end{aligned} \tag{3.13}$$

Hence, the following result:

Theorem 3.2. *The endemic equilibrium*

$$E_{C1} = (S^*, V^*, A^*, I^*, R^*)$$

of the COVID-19-only model (3.1) *has one unique endemic equilibrium if* $R_{C0} > 1$.

Theorem 3.3. *The endemic equilibrium*

$$E_{C1} = (S^*, V^*, A^*, I^*, R^*)$$

of the COVID-19-only model (3.1) *is globally asymptotically stable if* $R_{C0} > 1$.

Proof. The Lyapunov function $L_2(t)$ is given by

$$L_2 = S - S^* - S^* \ln \frac{S}{S^*} + V - V^* - V^* \ln \frac{V}{V^*} + A - A^* - A^* \ln \frac{A}{A^*} + \frac{\beta_c [S^* + (1-\theta) V^*]}{(\delta_2 + \varphi_2 + \mu) N^0} \left(I - I^* - I^* \ln \frac{I}{I^*} \right). \tag{3.14}$$

The derivative of $L_2(t)$ along the solutions of model (3.1) is as follows:

$$\dot{L}_2 = \left(1 - \frac{S^*}{S}\right)\dot{S} + \left(1 - \frac{V^*}{V}\right)\dot{V} + \left(1 - \frac{A^*}{A}\right)\dot{A} + \frac{\beta_c [S^* + (1-\theta) V^*]}{(\delta_2 + \varphi_2 + \mu) N^0} \left(1 - \frac{I^*}{I}\right)\dot{I}. \tag{3.15}$$

Let

$$x = \frac{S}{S^*}, \quad y = \frac{V}{V^*}, \quad g = \frac{A}{A^*}, \quad t = \frac{I}{I^*}, \tag{3.16}$$

we obtain

$$\begin{aligned} \dot{L}_2 =& (1 - \frac{1}{x})[\Lambda - \frac{\beta_c \varepsilon_1 A^* S^*}{N^0} xg - \frac{\beta_c \varepsilon_1 I^* S^*}{N^0} xt - (\mu + \tau) S^* x] \\ &+ \left(1 - \frac{1}{y}\right)[\tau S^* x - \frac{(1-\theta)\beta_c \varepsilon_1 A^* V^*}{N^0} yg \\ &- \frac{(1-\theta)\beta_c I^* V^*}{N^0} ty - \mu V^* y] + (1 - \frac{1}{g})[\frac{\beta_c \varepsilon_1 A^* S^*}{N^0} xg \\ &+ \frac{(1-\theta)\beta_c \varepsilon_1 A^* V^*}{N^0} yg + \frac{\beta_c I^* S^*}{N^0} xt + \frac{(1-\theta)\beta_c I^* V^*}{N^0} ty \\ &- (\rho + \varphi_3 + \mu) A^* g] + \frac{\beta_c [S^* + (1-\theta) V^*]}{(\delta_2 + \varphi_2 + \mu) N^0} \cdot \\ &\left(1 - \frac{1}{t}\right)[\rho A^* g - (\delta_2 + \varphi_2 + \mu) I^* t] \\ =& \Lambda + (\mu + \tau) S^* + \mu V^* + (\rho + \varphi_3 + \mu) A^* \\ &+ \frac{\beta_c [S^* + (1-\theta) V^*]}{N^0} I^* - \left(\mu S^* + \frac{\beta_c \varepsilon_1 A^* S^*}{N^0}\right) x - \Lambda \frac{1}{x} \\ &- \left(\mu V^* + \frac{(1-\theta)\beta_c \varepsilon_1 A^* V^*}{N^0}\right) y - \tau S^* \frac{x}{y} - \frac{\beta_c I^* S^*}{N^0} \frac{xt}{g} \\ &- \frac{(1-\theta)\beta_c I^* V^*}{N^0} \frac{ty}{g} - \frac{\beta_c [S^* + (1-\theta) V^*]}{(\delta_2 + \varphi_2 + \mu) N^0} \rho A^* \frac{g}{t} \\ =& \left(\mu S^* + \frac{\beta_c \varepsilon_1 A^* S^*}{N^0}\right)\left(2 - x - \frac{1}{x}\right) \\ &+ \left(\mu V^* + \frac{(1-\theta)\beta_c \varepsilon_1 A^* V^*}{N^0}\right)\left(3 - y - \frac{x}{y} - \frac{1}{x}\right) \\ &+ \frac{\beta_c I^* S^*}{N^0}\left(3 - \frac{xt}{g} - \frac{g}{t} - \frac{1}{x}\right) \\ &+ \frac{(1-\theta)\beta_c I^* V^*}{N^0}\left(4 - \frac{ty}{g} - \frac{g}{t} - \frac{x}{y} - \frac{1}{x}\right). \end{aligned} \tag{3.17}$$

Because the arithmetic mean is greater than or equal to the geometric mean,

$$\begin{aligned} &2-x-\frac{1}{x}\leq 0, \quad 3-y-\frac{x}{y}-\frac{1}{x}\leq 0,\\ &3-\frac{xt}{g}-\frac{g}{t}-\frac{1}{x}\leq 0, \quad 4-\frac{ty}{g}-\frac{g}{t}-\frac{x}{y}-\frac{1}{x}\leq 0. \end{aligned} \tag{3.18}$$

It can be verified that $\dot{L}_2 \leq 0$ for $R_{C0} > 1$. Hence, by the LaSalle's invariance principle [42], the endemic equilibrium E_{C1} of model (3.1) is global asymptotically stable when $R_{C0} > 1$. □

3.2. Malaria-only model

The malaria-only model is obtained by setting

$$V(t) = A(t) = I(t) = I_E(t) = 0$$

in (2.1). We have

$$\begin{cases} \dfrac{dS(t)}{dt} = \Lambda - \lambda_m S - \mu S, \\ \dfrac{dE(t)}{dt} = \lambda_m S - (\delta_1 + \varphi_1 + \mu) E, \\ \dfrac{dR(t)}{dt} = \varphi_1 E - \mu R, \\ \dfrac{dS_v(t)}{dt} = \Lambda_v - \lambda_v S_v - \mu_v S_v, \\ \dfrac{dE_v(t)}{dt} = \lambda_v S_v - (\alpha_v + \mu_v) E_v, \\ \dfrac{dI_v(t)}{dt} = \alpha_v E_v - \mu_v I_v, \end{cases} \tag{3.19}$$

where,

$$\lambda_m = \frac{\beta_m b I_v}{N}, \quad \lambda_v = \frac{\beta_v b E}{N}$$

and

$$N = S + E + R.$$

Consider the region

$$\Gamma_M = \left\{ (S, E, R, S_v, E_v, I_v) \in R_+^6 : N(t) \leq \frac{\Lambda}{\mu}, N_v(t) \leq \frac{\Lambda_v}{\mu_v} \right\}.$$

It can be shown that the region Γ_M is positively invariant.

3.2.1. Stability of the disease-free equilibrium

The disease-free equilibrium of the malaria-only model (3.19) is given by

$$E_{M0} = \left(S^0, E^0, R^0, S_v^0, E_v^0, I_v^0\right) = \left(\frac{\Lambda}{\mu}, 0, 0, \frac{\Lambda_v}{\mu_v}, 0, 0\right).$$

According to the next generation matrix method [41], the basic reproduction number is calculated as follows:

$$\mathcal{F} = \begin{pmatrix} \lambda_m S \\ \lambda_v S_v \\ 0 \end{pmatrix}, \quad \mathcal{V} = \begin{pmatrix} (\delta_1 + \varphi_1 + \mu) E \\ (\alpha_v + \mu_v) E_v \\ \mu_v I_v - \alpha_v E_v \end{pmatrix}.$$

Thus,

$$F = \begin{pmatrix} 0 & 0 & \beta_m b \\ \frac{\beta_v b \mu \Lambda_v}{\Lambda \mu_v} & 0 & 0 \\ 0 & 0 & 0 \end{pmatrix},$$

$$V = \begin{pmatrix} \delta_1 + \varphi_1 + \mu & 0 & 0 \\ 0 & \alpha_v + \mu_v & 0 \\ 0 & -\alpha_v & \mu_v \end{pmatrix}.$$

The basic reproduction number R_{M0} of the model (3.19) is the spectral radius of matrix FV^{-1}. Thus, R_{M0} is given by

$$R_{M0} = \sqrt{\frac{\Lambda_v \beta_m \beta_v b^2 \mu \alpha_v}{\Lambda \mu_v^2 (\delta_1 + \varphi_1 + \mu)(\alpha_v + \mu_v)}}.$$

Lemma 3.2. *[43, Theorem A.1] Given $a > 0, b > 0, c > 0$ and $d > 0$, all roots of the function*

$$f(x) = (x + a)(x + b)(x + c)(x + d) - e$$

are negative or have negative real parts if and only if $abcd > e$.

Theorem 3.4. *The disease-free equilibrium E_{M0} of the malaria-only model* (3.19) *is locally asymptotically stable if $R_{M0} < 1$, and unstable if $R_{M0} > 1$.*

Proof. The Jacobian matrix of model (3.19) at E_{M0} is given by

$$J(E_{M0}) = \begin{pmatrix} -\mu & 0 & 0 & 0 & 0 & -\beta_m b \\ 0 & -(\delta_1 + \varphi_1 + \mu) & 0 & 0 & 0 & \beta_m b \\ 0 & \varphi_1 & -\mu & 0 & 0 & 0 \\ 0 & -\frac{\Lambda_v \beta_v b \mu}{\Lambda \mu_v} & 0 & -\mu_v & 0 & 0 \\ 0 & \frac{\Lambda_v \beta_v b \mu}{\Lambda \mu_v} & 0 & 0 & -(\alpha_v + \mu_v) & 0 \\ 0 & 0 & 0 & 0 & \alpha_v & -\mu_v \end{pmatrix}. \tag{3.20}$$

The eigenvalues of the Jacobin matrix $J(E_{M0})$ include $-\mu$, $-\mu_v$. The other eigenvalues are the roots of the following equation:

$$\begin{aligned}|\lambda - J_1| &= \begin{vmatrix} \lambda + (\delta_1 + \varphi_1 + \mu) & 0 & -\beta_m b \\ -\frac{\Lambda_v \beta_v b \mu}{\Lambda \mu_v} & \lambda + (\alpha_v + \mu_v) & 0 \\ 0 & -\alpha_v & \lambda + \mu_v \end{vmatrix} \\ &= [\lambda + (\delta_1 + \varphi_1 + \mu)][\lambda + (\alpha_v + \mu_v)](\lambda + \mu_v) \\ &\quad - \frac{\Lambda_v \beta_m \beta_v b^2 \mu \alpha_v}{\Lambda \mu_v}. \end{aligned} \tag{3.21}$$

Due to the $R_{M0} < 1$, then

$$(\delta_1 + \varphi_1 + \mu)(\alpha_v + \mu_v)\mu_v > \frac{\Lambda_v \beta_m \beta_v b^2 \mu \alpha_v}{\Lambda \mu_v}.$$

According to Lemma 3.2, all the roots of the characteristic equation have negative real parts if R_{M0} <1. Hence, the disease-free equilibrium E_{M0} of the malaria-only model (3.19) is locally asymptotically stable when R_{M0} <1. □

3.2.2. Existence of the endemic equilibrium of the malaria-only model

By setting each of the equations of model (3.19) to zero, the endemic equilibrium is given by

$$E_{M1} = (S^*, E^*, R^*, S_v^*, E_v^*, I_v^*),$$

where

$$\begin{aligned} S^* &= \frac{\Lambda}{\lambda_m^* + \mu}, \quad E^* = \frac{\lambda_m^* S^*}{\delta_1 + \varphi_1 + \mu}, \quad R^* = \frac{\varphi_1 E^*}{\mu}, \\ S_v^* &= \frac{\Lambda_v}{\lambda_v^* + \mu_v}, \quad E_v^* = \frac{\lambda_v^* S_v^*}{\alpha_v + \mu_v}, \quad I_v^* = \frac{\alpha_v E_v^*}{\mu_v} \end{aligned} \tag{3.22}$$

and

$$\lambda_m^* = \beta_m b \frac{I_v^*}{S^* + E^* + R^*}.$$

From expressions (3.22), we obtain

$$\begin{aligned} N^* &= S^* + E^* + R^* \\ &= \frac{\Lambda}{\lambda_m^* + \mu} + \frac{\lambda_m^* \Lambda}{(\delta_1 + \varphi_1 + \mu)(\lambda_m^* + \mu)} \\ &\quad + \frac{\varphi_1 \lambda_m^* \Lambda}{\mu(\delta_1 + \varphi_1 + \mu)(\lambda_m^* + \mu)} \\ &= \frac{\Lambda[\mu(\delta_1 + \varphi_1 + \mu) + \lambda_m^*(\varphi_1 + \mu)]}{\mu(\delta_1 + \varphi_1 + \mu)(\lambda_m^* + \mu)}. \end{aligned} \tag{3.23}$$

After some little algebraic manipulations, we obtain

$$\begin{aligned} I_v^* &= \frac{\alpha_v \lambda_v^* \Lambda_v}{\mu_v(\alpha_v + \mu_v)(\lambda_v^* + \mu_v)} \\ &= \frac{\lambda_m^* \Lambda \Lambda_v \beta_v b \alpha_v}{\mu_v(\alpha_v + \mu_v)[\Lambda \beta_v b \lambda_m^* + \mu_v N^*(\delta_1 + \varphi_1 + \mu)(\lambda_m^* + \mu)]}. \end{aligned} \tag{3.24}$$

Substituting (3.23) and (3.24) into the expression for λ_m^*, we obtain

$$\begin{aligned} \lambda_m^* = &\frac{1}{\mu_v(\alpha_v + \mu_v)[\mu(\delta_1 + \varphi_1 + \mu) + \lambda_m^*(\varphi_1 + \mu)]} \\ &\frac{\lambda_m^* \mu^2 b^2 \Lambda_v \beta_m \beta_v \alpha_v (\delta_1 + \varphi_1 + \mu)(\lambda_m^* + \mu)}{[\lambda_m^* \mu b \Lambda \beta_v + \Lambda \mu_v [\mu(\delta_1 + \varphi_1 + \mu) + \lambda_m^*(\varphi_1 + \mu)]]}. \end{aligned} \tag{3.25}$$

After some lengthy algebraic manipulations, the endemic equilibria of the malaria-only model (3.19) satisfy the following polynomial in terms of λ_m^* given by

$$\lambda_m^* \left(A {\lambda_m^*}^2 + B \lambda_m^* + C \right) = 0, \tag{3.26}$$

where,

$$\begin{aligned} A =& \Lambda \mu_v (\alpha_v + \mu_v)(\varphi_1 + \mu)[\mu b \beta_v + \mu_v(\varphi_1 + \mu)], \\ B =& \Lambda \mu {\mu_v}^2 (\alpha_v + \mu_v)(\varphi_1 + \mu)(\delta_1 + \varphi_1 + \mu) \\ &+ \Lambda \mu \mu_v (\alpha_v + \mu_v)(\delta_1 + \varphi_1 + \mu)[\mu b \beta_v + \mu_v(\varphi_1 + \mu)] \\ &- \mu^2 b^2 \Lambda_v \beta_m \beta_v \alpha_v (\delta_1 + \varphi_1 + \mu), \\ C =& \Lambda \mu^2 {\mu_v}^2 (\alpha_v + \mu_v)(\delta_1 + \varphi_1 + \mu)^2 \\ &- \mu^3 b^2 \Lambda_v \beta_m \beta_v \alpha_v (\delta_1 + \varphi_1 + \mu) \\ =& \Lambda \mu^2 {\mu_v}^2 (\alpha_v + \mu_v)(\delta_1 + \varphi_1 + \mu)^2 \left(1 - R_{M0}^2\right). \end{aligned} \tag{3.27}$$

It is worth noting that the coefficient A is always positive and C is positive if $R_{M0} < 1$, and negative if $R_{M0} > 1$. Hence, we have established the following result:

Theorem 3.5. *The malaria-only model* (3.19) *has:*
(i) Precisely one unique endemic equilibrium if $C < 0 \Leftrightarrow R_{M0} > 1$*;*
(ii) Precisely one unique endemic equilibrium if $B < 0$ *and* $C = 0$ *or* $B^2 - 4AC = 0$*;*
(iii) Precisely two endemic equilibria if $C > 0, B < 0$ *and* $B^2 - 4AC > 0$*;*
(iv) No endemic equilibrium otherwise.

Case (iii) indicates the possibility of backward bifurcation in the model, and the disease may spread even though R_{M0} <1.

3.3. Malaria-COVID-19 model

The feasible region for model (2.1) is given by

$$\Gamma_{CM} = \Gamma_C \times \Gamma_M,$$

where Γ_C and Γ_M are defined in (3.1) and (3.19), respectively.

The disease-free equilibrium of model (2.1) is given by

$$\begin{aligned} E_0 &= (S, V, A, I, E, I_E, R, S_v, E_v, I_v) \\ &= (\frac{\Lambda}{\mu+\tau}, \frac{\Lambda\tau}{\mu(\mu+\tau)}, 0, 0, 0, 0, 0, \frac{\Lambda_v}{\mu_v}, 0, 0). \end{aligned} \tag{3.28}$$

From the basic reproduction number of the COVID-19-only and malaria-only sub-models, the basic reproduction number of the full model is given as

$$R_0 = max\{R_{C0}, R_{M0}\}. \tag{3.29}$$

Following Theorem 2 in [41], the model (2.1) has the following results:

Theorem 3.6. *The disease-free equilibrium of the full model* (2.1) *is locally asymptotically stable if* $R_0 < 1$*, and unstable if* $R_0 > 1$.

4. Optimal control model

To investigate the impact of intervention measures, we incorporate the following four controls into the full model (2.1):

u_1: Control against incident COVID-19 infection, such as vaccination;

u_2: Control against incident malaria infection, such as insecticide treatment of mosquito nets;

u_3: COVID-19 treatment control;

u_4: Malaria treatment control.

The controls u_1 and u_2 satisfy

$$0 \le u_1 \le 0.95$$

following the general efficacy of the COVID-19 vaccine [15],

$$0 \le u_2 \le 0.95.$$

The COVID-19 and malaria treatment controls u_3 and u_4 are bounded as follows:

$$0 \le u_3,\ u_4 \le 0.9.$$

The model (2.1) now reads

$$\begin{cases} \dfrac{dS(t)}{dt} = \Lambda - (1-u_2)\lambda_m S - (1-u_1)\lambda_c S - (\mu+\tau)S, \\ \dfrac{dV(t)}{dt} = \tau S - (1-\theta)(1-u_1)\lambda_c V - (1-u_2)\lambda_m V - \mu V, \\ \dfrac{dA(t)}{dt} = (1-u_1)\lambda_c[S + (1-\theta)V] - (\rho + u_3 + \mu)A, \\ \dfrac{dI(t)}{dt} = \rho A - \sigma_2(1-u_2)\lambda_m I - (\delta_2 + u_3 + \mu)I + u_4 I_E, \\ \dfrac{dE(t)}{dt} = (1-u_2)\lambda_m(S+V) - \sigma_1(1-u_1)\lambda_c E \\ \qquad\qquad - (\delta_1 + u_4 + \mu)E + u_3 I_E, \\ \dfrac{dI_E(t)}{dt} = \sigma_1(1-u_1)\lambda_c E + \sigma_2(1-u_2)\lambda_m I \\ \qquad\qquad - (\delta_3 + \mu + u_3 + u_4)I_E, \\ \dfrac{dR(t)}{dt} = u_4 E + u_3(A+I) - \mu R, \\ \dfrac{dS_v(t)}{dt} = \Lambda_v - (1-u_2)\lambda_v S_v - \mu_v S_v, \\ \dfrac{dE_v(t)}{dt} = (1-u_2)\lambda_v S_v - (\alpha_v + \mu_v)E_v, \\ \dfrac{dI_v(t)}{dt} = \alpha_v E_v - \mu_v I_v, \end{cases} \tag{4.1}$$

with initial conditions

$$\begin{aligned} &S(0) \ge 0, V(0) \ge 0, A(0) \ge 0, I(0) \ge 0, E(0) \ge 0, \\ &I_E(0) \ge 0, R(0) \ge 0, S_v(0) \ge 0, E_v(0) \ge 0, I_v(0) \ge 0. \end{aligned} \tag{4.2}$$

The following objective function is considered.

$$\begin{aligned} J(u_1, u_2, u_3, u_4) = \int_0^T (&C_1 A + C_2 I + C_3 E + C_4 I_E + C_5 N_v \\ &+ \frac{w_1}{2}u_1^2 + \frac{w_2}{2}u_2^2 + \frac{w_3}{2}u_3^2 + \frac{w_4}{2}u_4^2)\,dt, \end{aligned} \tag{4.3}$$

where T is the final time, $C_i, i = 1, \cdots, 5$ are positive weight constants, and $w_i, i = 1, \cdots, 4$ are weight constants for the strategies and treatments against proliferation of the COVID-19 and malaria. The goal is to find an optimal control, u_1^*–u_4^*, such that

$$J\left(u_1^*, u_2^*, u_3^*, u_4^*\right) = \min\left\{J\left(u_1^*, u_2^*, u_3^*, u_4^*\right) | u_1, u_2, u_3, u_4 \in U\right\}, \tag{4.4}$$

where

$$U = \left\{\left(u_1^*, u_2^*, u_3^*, u_4^*\right)\right\},$$

such that u_1^*–u_4^* are measurable with

$$0 \le u_1^* \le 0.95, 0 \le u_2^* \le 0.95, 0 \le u_3^* \le 0.9, 0 \le u_4^* \le 0.9$$

for $t \in [0, T]$ is the control set. The Hamiltonian is given by

$$\begin{aligned} H =& C_1 A + C_2 I + C_3 E + C_4 I_E + C_5 N_v + \frac{w_1}{2} u_1^2 + \frac{w_2}{2} u_2^2 \\ &+ \frac{w_3}{2} u_3^2 + \frac{w_4}{2} u_4^2 + \lambda_1 \dot{S} + \lambda_2 \dot{V} + \lambda_3 \dot{A} + \lambda_4 \dot{I} + \lambda_5 \dot{E} \\ &+ \lambda_6 \dot{I}_E + \lambda_7 \dot{R} + \lambda_8 \dot{S}_v + \lambda_9 \dot{E}_v + \lambda_{10} \dot{I}_v, \end{aligned} \tag{4.5}$$

where $\lambda_i, i = 1, \cdots, 10$ are the adjoint variables. Pontryagins maximum principle [44] is applied, such that there exist adjoint variables satisfying:

$$\begin{aligned} &\lambda'_1 = -\frac{\partial H}{\partial S}, \ \lambda'_2 = -\frac{\partial H}{\partial V}, \ \lambda'_3 = -\frac{\partial H}{\partial A}, \ \lambda'_4 = -\frac{\partial H}{\partial I}, \\ &\lambda'_5 = -\frac{\partial H}{\partial E}, \ \lambda'_6 = -\frac{\partial H}{\partial I_E}, \ \lambda'_7 = -\frac{\partial H}{\partial R}, \ \lambda'_8 = -\frac{\partial H}{\partial S_v}, \\ &\lambda'_9 = -\frac{\partial H}{\partial E_v}, \ \lambda'_{10} = -\frac{\partial H}{\partial I_v}. \end{aligned} \tag{4.6}$$

Writing (4.6) in details gives

$$\begin{aligned} \lambda_1' =& (1-u_1)\lambda_c\Big[(\lambda_1-\lambda_3)\Big(1-\frac{S}{N}\Big)+(1-\theta)\frac{V}{N}(\lambda_3-\lambda_2) \\ &+\sigma_1\frac{E}{N}(\lambda_6-\lambda_5)\Big]+(1-u_2)\lambda_m\Big[(\lambda_1-\lambda_5)\Big(1-\frac{S}{N}\Big) \\ &+\frac{V}{N}(\lambda_5-\lambda_2)+\sigma_2\frac{I}{N}(\lambda_6-\lambda_4)\Big] \\ &+(\mu+\tau)\lambda_1-\tau\lambda_2+(1-u_2)\lambda_v\frac{S_v}{N}(\lambda_9-\lambda_8), \\ \lambda_2' =& (1-u_1)\lambda_c\Big[\frac{S}{N}(\lambda_3-\lambda_1)+(1-\theta)\Big(1-\frac{V}{N}\Big)(\lambda_2-\lambda_3) \\ &+\sigma_1\frac{E}{N}(\lambda_6-\lambda_5)\Big]+(1-u_2)\lambda_m\Big[\frac{S}{N}(\lambda_5-\lambda_1) \\ &+\Big(1-\frac{V}{N}\Big)(\lambda_2-\lambda_5)+\sigma_2\frac{I}{N}(\lambda_6-\lambda_4)\Big] \\ &+\mu\lambda_2+(1-u_2)\lambda_v\frac{S_v}{N}(\lambda_9-\lambda_8), \\ \lambda_3' =& (1-u_1)\frac{\beta_c\varepsilon_1-\lambda_c}{N}\Big[S(\lambda_1-\lambda_3)+(1-\theta)V(\lambda_2-\lambda_3) \\ &+\sigma_1E(\lambda_5-\lambda_6)\Big]+(1-u_2)\lambda_m\Big[\frac{S}{N}(\lambda_5-\lambda_1) \\ &+\frac{V}{N}(\lambda_5-\lambda_2)+\sigma_2\frac{I}{N}(\lambda_6-\lambda_4)\Big]+\lambda_3(\rho+u_3+\mu) \\ &-\lambda_4\rho-\lambda_7u_3+(1-u_2)\lambda_v\frac{S_v}{N}(\lambda_9-\lambda_8)-C_1, \\ \lambda_4' =& (1-u_1)\frac{\beta_c-\lambda_c}{N}\Big[S(\lambda_1-\lambda_3)+(1-\theta)V(\lambda_2-\lambda_3) \\ &+\sigma_1E(\lambda_5-\lambda_6)\Big]+(1-u_2)\lambda_m\Big[\frac{S}{N}(\lambda_5-\lambda_1) \\ &+\frac{V}{N}(\lambda_5-\lambda_2)+\sigma_2\Big(1-\frac{I}{N}\Big)(\lambda_4-\lambda_6)\Big]-C_2 \\ &+\lambda_4(\delta_2+u_3+\mu)-\lambda_7u_3+(1-u_2)\lambda_v\frac{S_v}{N}(\lambda_9-\lambda_8), \\ \lambda_5' =& -C_3+(1-u_1)\lambda_c\Big[\frac{S}{N}(\lambda_3-\lambda_1)+(1-\theta)\frac{V}{N}(\lambda_3-\lambda_2) \\ &+\sigma_1\Big(1-\frac{E}{N}\Big)(\lambda_5-\lambda_6)\Big]+(1-u_2)\lambda_m\Big[\frac{S}{N}(\lambda_5-\lambda_1) \\ &+\frac{V}{N}(\lambda_5-\lambda_2)+\sigma_2\frac{I}{N}(\lambda_6-\lambda_4)\Big] \\ &-\lambda_7u_4+(1-u_2)\frac{\beta_vb-\lambda_v}{N}S_v(\lambda_8-\lambda_9), \\ \lambda_6' =& (1-u_1)\frac{\beta_c-\lambda_c}{N}\Big[S(\lambda_1-\lambda_3)+(1-\theta)V(\lambda_2-\lambda_3) \\ &+\sigma_1E(\lambda_5-\lambda_6)\Big]+(1-u_2)\lambda_m\Big[\frac{S}{N}(\lambda_5-\lambda_1) \\ &+\frac{V}{N}(\lambda_5-\lambda_2)+\sigma_2\frac{I}{N}(\lambda_6-\lambda_4)\Big]-\lambda_4u_4-\lambda_5u_3 \\ &+\lambda_6(\delta_3+\mu+u_3+u_4)-C_4 \\ &+(1-u_2)\frac{\beta_vb-\lambda_v}{N}S_v(\lambda_8-\lambda_9), \\ \lambda_7' =& (1-u_1)\frac{\lambda_c}{N}\Big[S(\lambda_3-\lambda_1)+(1-\theta)V(\lambda_3-\lambda_2) \\ &+\sigma_1E(\lambda_6-\lambda_5)\Big]+(1-u_2)\frac{\lambda_m}{N}\Big[S(\lambda_5-\lambda_1) \\ &+V(\lambda_5-\lambda_2)+\sigma_2I(\lambda_6-\lambda_4)\Big] \\ &+\mu\lambda_7+(1-u_2)\lambda_v\frac{S_v}{N}(\lambda_9-\lambda_8), \\ \lambda_8' =& -C_5+(1-u_2)\lambda_v(\lambda_8-\lambda_9)+\lambda_8\mu_v, \\ \lambda_9' =& -C_5+\lambda_9(\alpha_v+\mu_v)-\lambda_{10}\alpha_v, \\ \lambda_{10}' =& -C_5+(1-u_2)\frac{\beta_mb-\lambda_m}{N}\Big[S(\lambda_1-\lambda_5) \\ &+V(\lambda_2-\lambda_5)+\sigma_2I(\lambda_4-\lambda_6)\Big]+\lambda_{10}\mu_v. \end{aligned} \tag{4.7}$$

The necessary and sufficient optimality conditions are

$$\begin{aligned} 0 =& \frac{\partial H}{\partial u_1} = w_1u_1+\lambda_c\Big[S(\lambda_1-\lambda_3)+(1-\theta)V(\lambda_2-\lambda_3) \\ &+\sigma_1E(\lambda_5-\lambda_6)\Big], \\ 0 =& \frac{\partial H}{\partial u_2} = w_2u_2+\lambda_m\Big[(S+V)(\lambda_1+\lambda_2-\lambda_5) \\ &+\sigma_2I(\lambda_4-\lambda_6)\Big]+\lambda_vS_v(\lambda_8-\lambda_9), \\ 0 =& \frac{\partial H}{\partial u_3} = w_3u_3+A(\lambda_7-\lambda_3)+I(\lambda_7-\lambda_4)+I_E(\lambda_5-\lambda_6), \\ 0 =& \frac{\partial H}{\partial u_4} = w_4u_4+E(\lambda_7-\lambda_5)+I_E(\lambda_4-\lambda_6). \end{aligned} \tag{4.8}$$

Therefore, the optimal controls are given

$$
\begin{aligned}
u_1^* &= \max\left\{0, \min\left(1, \frac{\lambda_c\left[S\left(\lambda_3-\lambda_1\right)+(1-\theta)V\left(\lambda_3-\lambda_2\right)+\sigma_1 E\left(\lambda_6-\lambda_5\right)\right]}{w_1}\right)\right\},\\
u_2^* &= \max\left\{0, \min\left(1,\right.\right.\\
&\quad \left.\left.\frac{\lambda_m\left[(S+V)\left(\lambda_5-\lambda_1-\lambda_2\right)+\sigma_2 I\left(\lambda_6-\lambda_4\right)\right]+\lambda_v S_v\left(\lambda_9-\lambda_8\right)}{w_2}\right)\right\},\\
u_3^* &= \max\left\{0, \min\left(1, \frac{A\left(\lambda_3-\lambda_7\right)+I\left(\lambda_4-\lambda_7\right)+I_E\left(\lambda_6-\lambda_5\right)}{w_3}\right)\right\},\\
u_4^* &= \max\left\{0, \min\left(1, \frac{E\left(\lambda_5-\lambda_7\right)+I_E\left(\lambda_6-\lambda_4\right)}{w_4}\right)\right\}.
\end{aligned}
\tag{4.9}
$$

5. Numerical simulations

To verify the results in the previous analysis, a numerical simulation of model (2.1) is carried out. The parameter values in Table 2 refer to a large number of literatures. In the absence of reference values, we make assumptions based on the actual situation. The initial value conditions of the model (2.1) are as follows:

$$S = 2500,\ V = 166,\ A = 15,\ I = 8,\ E = 11,$$
$$I_E = 3,\ R = 50,\ S_v = 10000,\ E_v = 8,\ I_v = 10.$$

We search the data of confirmed cases in South Africa in the early stage of the outbreak of COVID-19, and use Matlab to model fit the data. Data from the WHO website.

The period of the fitting covered 100 days, from March 6, 2020 to June 16, 2020. The "20" in Figure 3 represents the 20th day from March 6, 2020, and so on. The results are presented in Figure 3, from which it can be intuitively seen that our model fits well to the data set.

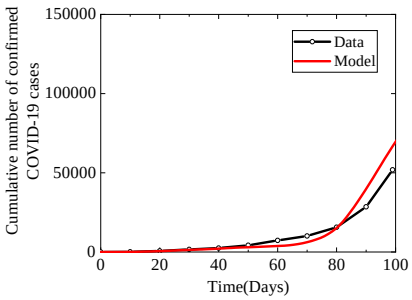

Figure 3. Model fitting diagram.

5.1. Sensitivity analysis

Understanding the relative importance of parameters can help to develop effective intervention strategies to control disease spread. Forward sensitivity analysis plays an important role in determining the relative importance of each parameter in disease epidemics and quantifies the impact of parameter variations. When R_{C0} and R_{M0} are response functions, we study the impact of parameters on R_{C0} and R_{M0}, respectively. In this section, we use the formula

$$S_\omega = \frac{\omega}{R_0}\frac{\partial R_0}{\partial \omega}$$

for analysis.

As can be seen from Table 3, when the COVID-19 associated with the basic reproduction number R_{C0} is used as a response function, the effective contact rate for the COVID-19 transmission (β_c, positively correlated) and the vaccine efficacy against COVID-19 (θ, negatively correlated), as well as the COVID-19 vaccination rate (τ, negatively correlated), dominate the disease dynamics. Furthermore, parameters $\delta_2, \varphi_2, \varphi_3$ (negatively correlated) and ε_1, ρ (positively correlated) also dominate the disease dynamics. These index values further indicate that if $\beta_c, \mu, \varepsilon_1, \rho$ increase or decrease by 10%, R_{C0} increases or decreases by 10%, 0.073%, 3.461%, and 0.708%, respectively. But on the other hand, the index for parameters $\varphi_2, \varphi_3, \delta_2, \theta$, and τ illustrates that increasing their values by 10% will decrease the values of reproduction number R_{C0} by 3.884%, 4.165%, 2.648%, 39.578%, and 0.084%, respectively.

Table 3. Sensitivity indices of the reproduction number R_{C0} against parameters.

Parameter	S.Index	Value	Parameter	S.Index	Value
β_c	S_{β_c}	1	μ	S_μ	0.0073
ε_1	S_{ε_1}	0.3461	φ_2	S_{φ_2}	-0.3884
ρ	S_ρ	0.0708	φ_3	S_{φ_3}	-0.4165
θ	S_θ	-3.9578	δ_2	S_{δ_2}	-0.2648
τ	S_τ	-0.0084			

Therefore, in order to effectively mitigate the transmission of COVID-19 in the population, the COVID-19 infection rate should be reduced first. In conjunction with the relevant policies, the populace should take appropriate protective measures to reduce the risk of infection. At the same time, effective vaccination can provide the public with physical immunity. This makes people less likely to get sick, which in turn reduces the infection rate β_c.

In Table 4, using the malaria associated with the basic reproduction number R_{M0} as a response function, the parameters $\Lambda_v, \beta_m, \beta_v, b, \alpha_v$ and μ have a positive effect on R_{M0}, which describe that the growth or decay of these parameters, say by 10%, will increase or decrease R_{M0} by 5%, 5%, 5%, 10%, 1.241%, and 4.995%, respectively. But the index for parameters $\Lambda, \mu_v, \varphi_1$ and δ_1 illustrates that increasing their values by 10% will decrease the values of R_{M0} by 5%, 11.241%, 4.757%, and 0.238%, respectively. These need to be achieved by comprehensive preventive measures and adequate medical resources. Second, mosquito control cannot be ignored. This requires spraying insecticides and hanging mosquito nets to reduce mosquito bites.

Table 4. Sensitivity indices of the reproduction number R_{M0} against parameters.

Parameter	S.Index	Value	Parameter	S.Index	Value
Λ	S_Λ	-0.5	Λ_v	S_{Λ_v}	0.5
β_m	S_{β_m}	0.5	β_v	S_{β_v}	0.5
b	S_b	1	α_v	S_{α_v}	0.1241
μ	S_μ	0.4995	μ_v	S_{μ_v}	-1.1241
φ_1	S_{φ_1}	-0.4757	δ_1	S_{δ_1}	-0.0238

The analysis of the basic reproduction number is crucial as the R_0 value is highly significant in determining the state of an epidemic. We study the effect of two parameters on the basic reproduction number when

$$R_0 = max\{R_{C0}, R_{M0}\} = R_{C0} = 1.7813.$$

Figure 4a shows that with the increase in the infection rate β_c, the R_0 value increases and decreases with the increase in vaccination rate τ. In Figure 4b, we clearly witness the decrease in the R_0 value with the decrease in the infection rate β_c and rate of onset of symptoms ρ values. Figure 4c shows that R_0 decreases with increase in vaccination rate τ and decrease in symptom onset rate ρ. The results indicate that vaccination provides protection to the population, resulting in a reduced probability of contracting the disease and a shorter recovery time for infected people. Thus, the reduction of β_c and ρ values is achieved. The decrease in the R_0 value also suggests that vaccination reduces the number of co-infections and the burden of health care. Additionally, we learn the range of these parameters when the R_0 value with below 1, which can indicate a direction for disease control.

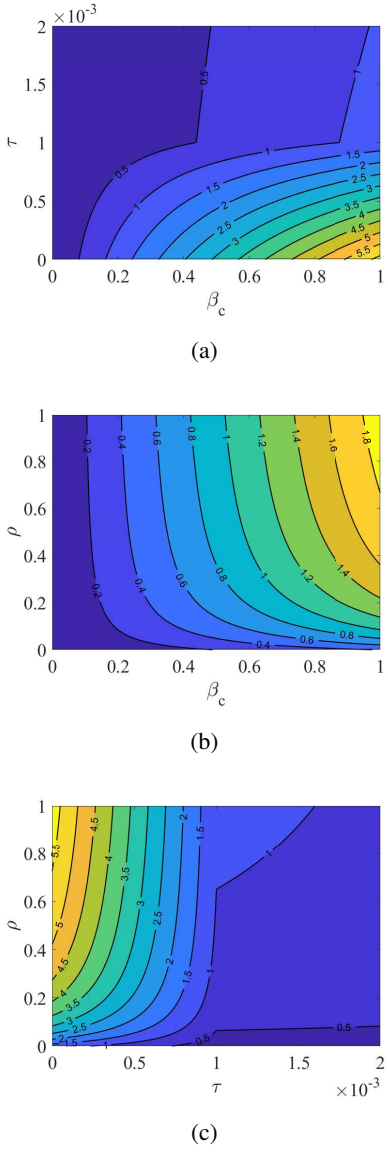

Figure 4. Effects of (a) β_c, τ, (b) β_c, ρ, and (c) τ, ρ on the reproduction number.

5.2. *Stability of equilibrium points*

In Figures 5–8, we plot the time series of sub-models and full model for parameter values given in Table 2, and verify the stability of equilibria. Figure 5 simulates the stability of the disease-free equilibrium of model (3.1). Other values of parameters are the same as in Table 2 except $\beta_c = 0.18$, then

$$R_{C0} = 0.874 < 1,$$

satisfying the condition of Theorem 3.1. It can be seen from Figure 5 that when t tends to infinity, the number of asymptomatic infectious individuals A and symptomatic infectious individuals I both tend to zero, indicating the spread of the disease is under control, which is consistent with the conclusion of Theorem 3.1.

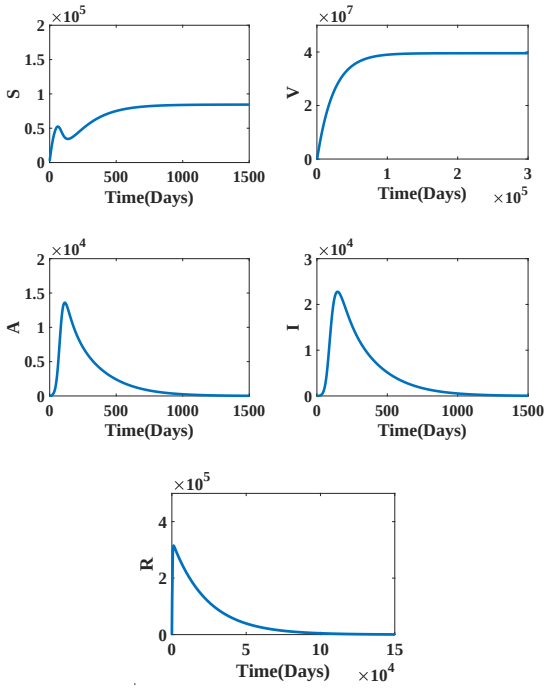

Figure 5. Stability of disease-free equilibrium of model (3.1).

Figure 6 simulates the stability of the endemic equilibrium of model (3.1). There

$$\beta_c = 0.4531$$

and other parameters are the same as in Table 2. Then, the

$$R_{C0} = 2.2 > 1$$

satisfies the conditions of Theorem 3.3. As shown in Figure 6, when t tends to infinity, the numbers of A and I are both greater than zero, indicating that humans will continue to be attacked by disease, which is also consistent with the conclusion of Theorem 3.3.

In a similar way, we simulate the stability of the disease-free equilibrium of models (2.1) and (3.19) in Figures 7 and 8, respectively, which verifies the correctness of Theorems 3.4 and 3.6.

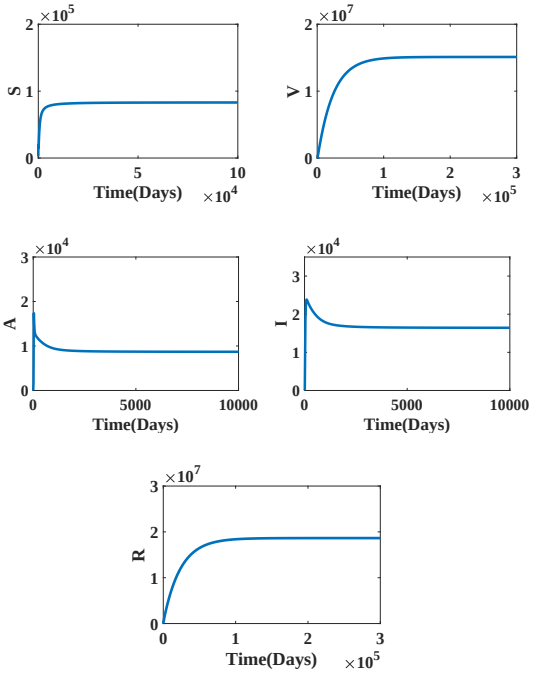

Figure 6. Stability of endemic equilibrium of model (3.1).

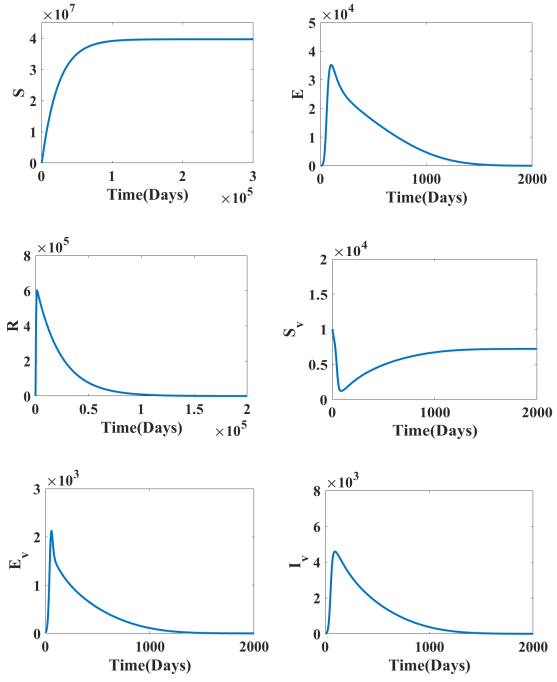

Figure 7. Stability of disease-free equilibrium of model (3.19).

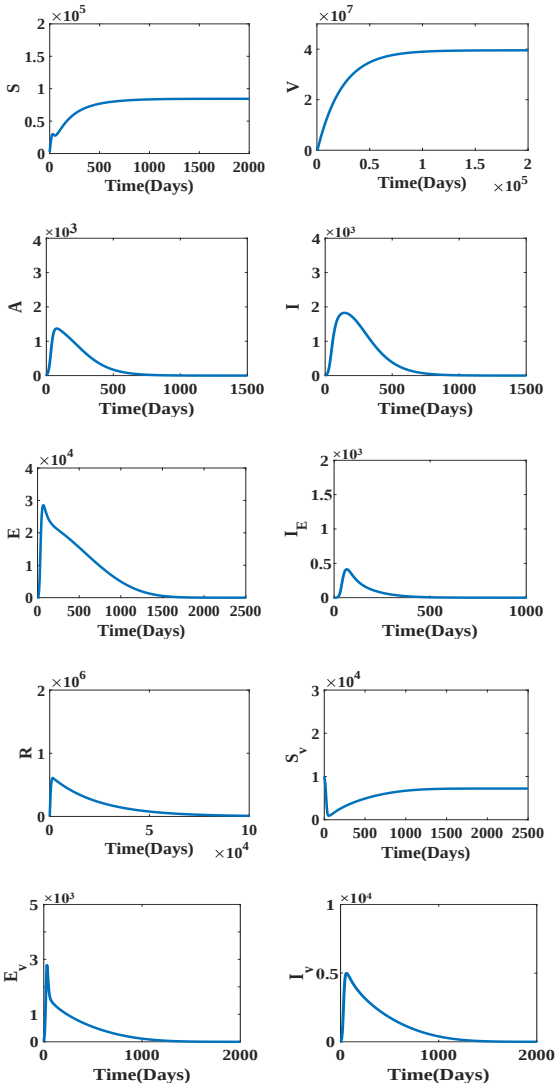

Figure 8. Stability of disease-free equilibrium of model (2.1).

5.3. Impact of several parameters on disease prevalence

The impacts of key parameters τ, θ, and ρ on variation in the co-infected population are shown in Figure 9. In Figure 9a, the co-infected population has been plotted for different vaccination rates τ, and it is clearly shown that the number of co-infected population decreases with the increase of vaccination rate. Set

$$\tau_{max} = 0.02$$

in drawing [37]. Figure 9b shows the trajectories of the co-infected population for different values of the vaccine efficacy θ. The larger the value of θ, the smaller the size of the co-infected group. Therefore, improving the vaccination rate and efficacy of vaccines can reduce the number of co-infections. In Figure 9c, the co-infected population has been illustrated for different values of symptom occurrence rates ρ. It is obvious from the figure that the co-infected population increases with the increase in symptom occurrence rate, so we should pay attention to the asymptomatic infected class and improve their recovery rate.

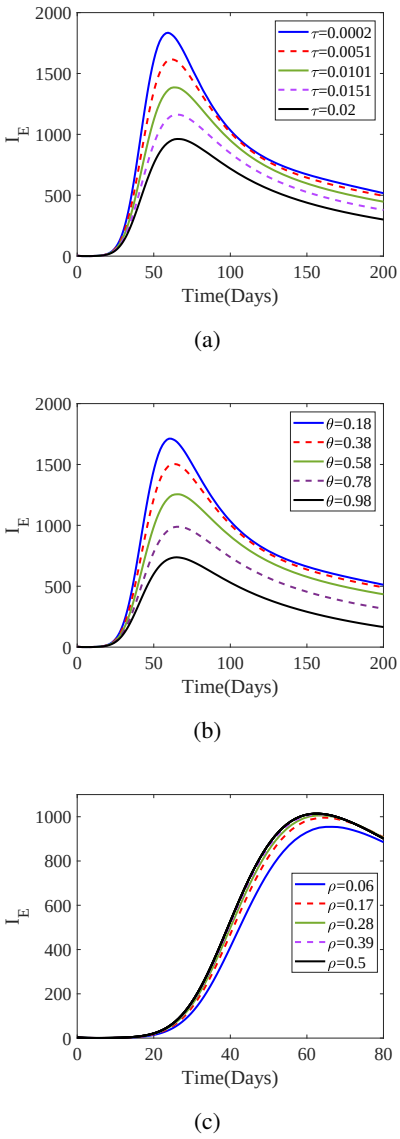

Figure 9. Effects of different (a) τ, (b) θ, and (c) ρ values on the number of co-infected population.

5.4. *Impacts of vaccination rate and efficacy of vaccine on co-infection*

Co-infected individuals have been presented in Figure 10 by varying the vaccination rate and vaccine efficacy at the same time. Figure 10 is drawn under the condition of low recovery rates. Let

$$\varphi_1 = 0.01, \quad \varphi_2 = 0.015, \quad \varphi_3 = 0.03, \quad \text{and} \quad \beta_c = 0.18,$$

then

$$R_0 = 1.2085 > 1.$$

If we increase the vaccination rate together with the vaccine efficacy, the number of co-infected people will gradually decrease. This suggests that active vaccination with effective vaccines can reduce the scale of an outbreak during an epidemic when the recovery rate is reduced due to the shortage of medical resources.

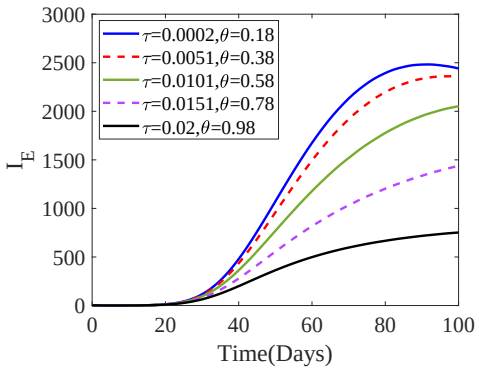

Figure 10. Effect of effective vaccination on the number of co-infected population.

In Figure 11, we hypothesize the effects of the following three situations on: co-infected population:

(1) Low vaccination rate and high vaccine efficacy;

(2) High vaccination rate and low vaccine efficacy;

(3) Low vaccination rate and low vaccine efficacy.

Other values of parameters are the same as in Table 2, except τ and θ. Through the two graphs in Figure 11, we can find that the curves of co-infected people basically coincide in the cases of (1) and (2), while in the case of (3), the number of co-infected population is much larger than the previous two cases.

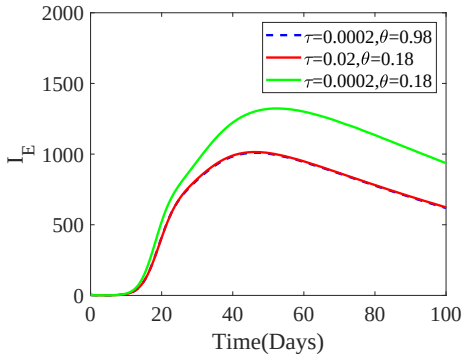

(a)

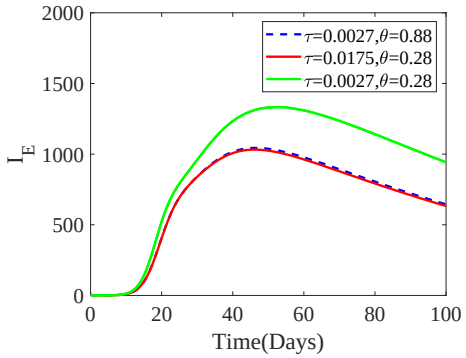

(b)

Figure 11. Effect of three situations on the number of co-infected population.

5.5. *Optimal control model simulation*

To support the analytical results, the optimal control model (4.1) is simulated using the model parameter values in Table 2. The balancing factors are assumed as follows: $C_1 = C_2 = C_3 = 2, C_4 = C_5 = 1$. The weight constants are set as follows: $w_1 = 1500, w_2 = 1000, w_3 = 1200$, and $w_4 = 900$.

5.5.1. Strategy A: COVID-19 prevention and treatment ($u_1 \neq 0, u_3 \neq 0, u_2 = u_4 = 0$)

The control model (4.1) is simulated when strategy A is implemented. The results of this strategy are shown in Figure 12a–c, respectively. When this intervention strategy is implemented, the number of symptomatic individuals I drastically decreases (Figure 12a). Interestingly, strategy A increases the number of individuals infected with malaria (Figure 12b). In other words, the implementation of strategy

A has prevented the progress of activities to control the spread of malaria, which conforms to the actual situation during the COVID-19 epidemic [7]. Many key activities are not effectively implemented, such as insecticide treatment of mosquito nets, chemical prevention for pregnant women and young children, and reduced access to effective antimalarial drugs. This means that tracking, treating, and controlling malaria are much more difficult than before. Also, it is worth noting that strategy A also has a positive population level impact on the number of individuals co-infected with COVID-19 and malaria (Figure 12c). The control profile depicted in Figure 12d shows that prevention is at optimal from the onset of the implementation and drops at around 100 days, while COVID-19 treatment drops at around 110 days.

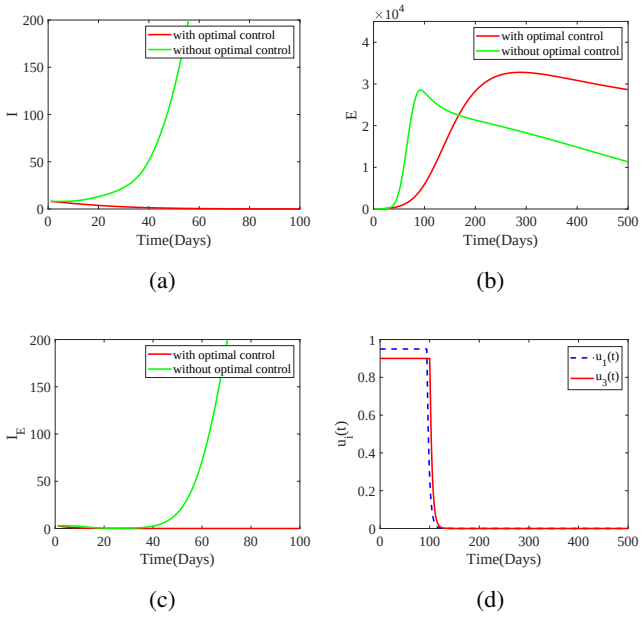

Figure 12. Impact of strategy A on individuals in (a) I, (b) E, and (c) I_E epidemiological class and (d) control profile for strategy A.

5.5.2. Strategy B: malaria prevention and treatment ($u_2 \neq 0, u_4 \neq 0, u_1 = u_3 = 0$)

Optimal control simulations of strategy B for model (4.1) are implemented. This strategy B reduces new cases of COVID-19, malaria, and co-infections. It is worth noting that strategy B delays the emergence of the peak of COVID-19 infection and lengthens the entire infection cycle. Moreover, this strategy also decreases cases of vector infections, thereby significantly reducing the infectious vector population (Figure 13d). The control profile for this control strategy is given in Figure 13e. The control profile shows that malaria treatment is at its peak within 10 to 80 days, drops and then rises again, and reaches about 0.07 and then drops slowly for the remaining days of the simulation, while prevention do not start to work until about 19 days, and then there is a little bump at about 200 days.

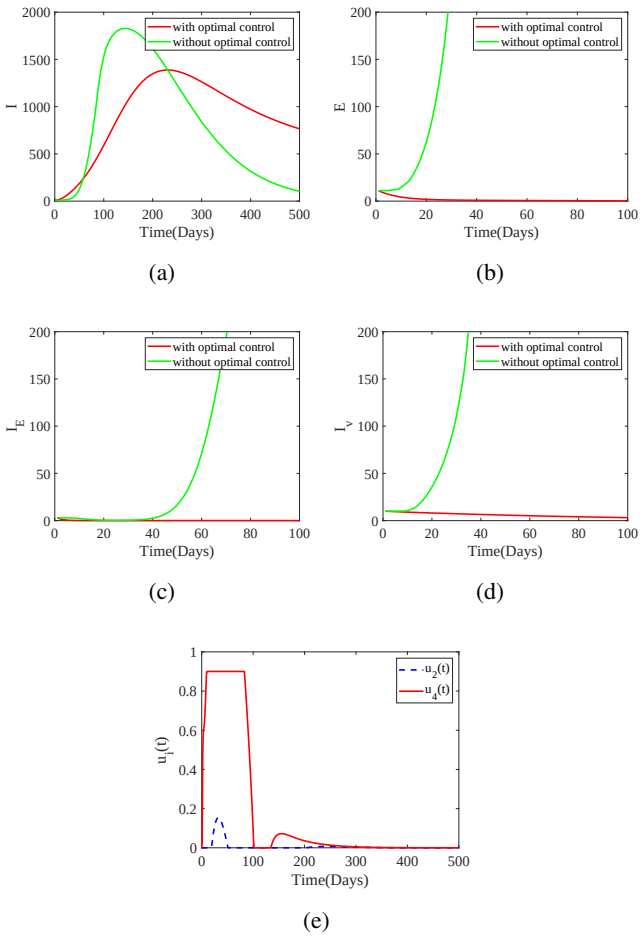

Figure 13. Impact of strategy B on individuals in (a) I, (b) E, (c) I_E, and (d) I_v epidemiological class and (e) control profile for strategy B.

6. Conclusions

The burden of malaria on human health has persisted for many years, especially in endemic areas. The symptoms of COVID-19 are similar to those of malaria, and there

is extensive geographic overlap. Besides, the COVID-19 pandemic has reversed progress on malaria. Thus, co-infection is a double whammy. In order to reduce the human burden of malaria and COVID-19, research on the co-infection of these diseases is particularly needed. In this work, a co-infection model of COVID-19 and malaria is constructed, which includes asymptomatic individuals infected with COVID-19. Vaccination and its timeliness are included in the model, as vaccination is an important measure to protect people from infectious diseases. We investigate the influence of vaccination on the co-infection of malaria and COVID-19, which creates a novel and more epidemiologically realistic model. This study seems to be the first of its kind to study the effect of vaccination on COVID-19 and malaria co-dynamics in detail. The theoretical analysis results are as follows:

(1) The disease-free equilibria of the sub-models are shown to be locally asymptotically stable when the respective reproduction numbers are below unity.

(2) When $R_{C0} > 1$, the COVID-19-only sub-model has a globally asymptotically stable endemic equilibrium.

(3) Compared with literature [13], the number of endemic equilibrium of the malaria sub-model is theoretically discussed. There is a possibility of backward bifurcation in this model, and although $R_{M0} < 1$ is necessary, it is not sufficient to eliminate the disease.

(4) The disease-free equilibrium of the co-infection model is locally asymptotically stable whenever the reproduction number

$$R_0 = max\{R_{C0}, R_{M0}\}$$

is less than unity.

The simulations of the stability of the disease-free equilibrium and endemic equilibrium verify the correctness of the theoretical analysis. The influence of important parameters on the basic reproduction number is numerically analyzed. The effects of different vaccination rates, vaccine efficacy and symptoms onset rates on co-infected individuals are also analyzed. In addition, the question of how the vaccination rate and efficacy affect the number of co-infected people is explored. The simulation results are as follows:

(1) The key parameters that dominate the disease dynamics are $\beta_c, \beta_m, \beta_v, \theta, \varphi_2, \varphi_3, \delta_2, \varphi_1, \delta_1, b, \tau$ (see Table 1 for parameter description).

(2) From the numerical results of sensitivity analysis, it is necessary to reduce the spread of these two diseases and increase effective vaccine management in order to curb the spread of the epidemic.

(3) The scale of the co-infected population decreases with the increase of vaccination rate and efficacy and increases with the increase of symptoms onset rate. Therefore, it is important to detect and treat asymptomatic individuals before they become symptomatic.

(4) When the recovery rate is low, that is, the medical resources are relatively tight, the influence of accepting effective vaccines actively on the co-infected population is simulated. Actively accepting effective vaccines (high vaccination rate and effectiveness) is helpful to reduce the number of co-infections and control the spread of diseases.

(5) A simple simulation of the three hypothetical situations in the paper aims to demonstrate that lack of effective vaccine vaccination will be detrimental to the control of co-infection of COVID-19 and malaria.

Next, based on the direction of future studies pointed out in literature [13], this paper adopts strategies different from those in literature [13]. After simulation of combination strategies, the results show that:

(1) Each strategy can reduce the burden of co-infection. Strategy B is more effective than strategy A.

(2) The implementation of strategy A reduces the number of individuals infected with COVID-19 but increases the number of malaria cases. In contrast, the use of strategy B results in a reduction in the number of individuals infected with both malaria and COVID-19.

(3) Strategy B reduces the peak value of COVID-19 infection but delays the occurrence of the peak value, indicating a trend toward a longer infection cycle.

(4) The use of strategy B reduces the number of vectors.

The findings suggest that if prevention and treatment for malaria infection are neglected, the disease will spread more widely. Therefore, other infectious diseases must not be neglected during the COVID-19 pandemic, and appropriate preventive measures and treatment services must be taken. These results provide insight into the impact of the implementation of one strategy on the other.

While this study provides further analysis for the transmission dynamics of malaria and COVID-19, this study can be extended. We explored the impact of vaccination on COVID-19-malaria co-infection, but the model did not take into account people's different attitudes towards vaccination. The co-infection model can be analyzed in the future based on different vaccination attitudes, or other extensions can be made, such as incorporating virus variation and stratifying the population by age.

Acknowledgments

This work was supported by The National Natural Science Foundation of China (11971278) and the Fund for Shanxi 1331KIRT.

Conflict of interest

The authors declare that they have no competing interests in this paper.

References

1. L. Wang, Z. D. Teng, T. L. Zhang, Threshold dynamics of a malaria transmission model in periodic environment, *Commun. Nonlinear Sci. Numer. Simul.*, **18** (2013), 1288–1303. https://doi.org/10.1016/j.cnsns.2012.09.007
2. Z. Mukandavire, A. B. Gumel, W. Garira, J. M. Tchuenche, Mathematical analysis of a model for HIV-malaria co-infection, *Math. Biosci. Eng.*, **6** (2009), 333–362. https://doi.org/10.3934/mbe.2009.6.333
3. X. R. Dong, X. Zhang, M. Y. Wang, L. W. Gu, J. Li, M. X. Gong, Heparin-decorated nanostructured lipid carriers of artemether-protoporphyrin IX-transferrin combination for therapy of malaria, *Int. J. Pharm.*, **605** (2021), 120813. https://doi.org/10.1016/j.ijpharm.2021.120813
4. L. Xue, C. A. Manore, P. Thongsripong, J. M. Hyman, Two-sex mosquito model for the persistence of Wolbachia, *J. Biol. Dyn.*, **11** (2017), 216–237. https://doi.org/10.1080/17513758.2016.1229051
5. P. Chanda-Kapata, N. Kapata, A. Zumla, COVID-19 and malaria: a symptom screening challenge for malaria endemic countries, *Int. J. Infect. Dis.*, **94** (2020), 151–153. https://doi.org/10.1016/j.ijid.2020.04.007
6. J. Nachega, M. Seydi, A. Zumla, The late arrival of coronavirus disease 2019 (COVID-19) in Africa: mitigating pan-continental spread, *Clin. Infect. Dis.*, **71** (2020), 875–878. https://doi.org/10.1093/cid/ciaa353
7. J. Hopman, B. Allegranzi, S. Mehtar, Managing COVID-19 in low- and middle-income countries, *JAMA*, **323** (2020), 1549–1550. https://doi.org/10.1001/jama.2020.4169
8. J. R. Gutman, N. W. Lucchi, P. T. Cantey, L. C Steinhardt, A. M Samuels, M. L. Kamb, et al., Malaria and parasitic neglected tropical diseases: potential syndemics with COVID-19? *Amer. J. Trop. Med. Hyg.*, **103** (2020), 572–577. https://doi.org/10.4269/ajtmh.20-0516
9. C. Y. Chiang, A. E. Sony, Tackling the threat of COVID-19 in Africa: an urgent need for practical planning, *Int. J. Tuberc. Lung. Dis.*, **24** (2020), 541–542. https://doi.org/10.5588/ijtld.20.0192
10. M. Gilbert, G. Pullano, F. Pinotti, E. Valdano, C. Poletto, P. Y. Boëlle, et al., Preparedness and vulnerability of African countries against importations of COVID-19: a modelling study, *Lancet*, **395** (2020), 871–877. https://doi.org/10.1016/S0140-6736(20)30411-6
11. V. Quaresima, M. M. Naldini, D. M. Cirillo, The prospects for the SARS-CoV-2 pandemic in Africa, *EMBO Mol. Med.*, **12** (2020), e12488. https://doi.org/10.15252/emmm.202012488
12. M. Majumder, P. K. Tiwari, S. Pal, Impact of nonlinear infection rate on HIV/AIDS considering prevalence-dependent awareness, *Math. Methods Appl. Sci.*, **46** (2023), 3821–3848. https://doi.org/10.1002/mma.8723

13. S. Y. Tchoumi, M. L. Diagne, H. Rwezaura, J. M. Tchuenche, Malaria and COVID-19 co-dynamics: a mathematical model and optimal control, *Appl. Math. Model.*, **99** (2021), 294–327. https://doi.org/10.1016/j.apm.2021.06.016

14. M. M. Ojo, E. F. D. Goufo, The impact of COVID-19 on a malaria dominated region: a mathematical analysis and simulations, *Alex. Eng. J.*, **65** (2023), 23–39. https://doi.org/10.1016/j.aej.2022.09.045

15. B. Yang, Z. H. Yu, Y. L. Cai, The impact of vaccination on the spread of COVID-19: studying by a mathematical model, *Phys. A*, **590** (2022), 126717. https://doi.org/10.1016/j.physa.2021.126717

16. B. J. Nath, K. Dehingia, V. N. Mishra, Y. M. Chu, H. K. Sarmah, Mathematical analysis of a within-host model of SARS-CoV-2, *Adv. Differ. Equations*, **2021** (2021), 13. https://doi.org/10.1186/s13662-021-03276-1

17. M. A. Rasheed, S. Raza, A. Zohaib, M. I. Riaz, A. Amin, M. Awais, et al., Immunoinformatics based prediction of recombinant multi-epitope vaccine for the control and prevention of SARS-CoV-2, *Alex. Eng. J.*, **60** (2021), 3087–3097. https://doi.org/10.1016/j.aej.2021.01.046

18. Z. H. Shen, Y. M. Chu, M. A. Khan, S. Muhammad, O. A. Al-Hartomy, M. Higazy, Mathematical modeling and optimal control of the COVID-19 dynamics, *Results Phys.*, **31** (2021), 105028. https://doi.org/10.1016/j.rinp.2021.105028

19. Y. M. Chu, A. Ali, M. A. Khan, S. Islam, S. Ullah, Dynamics of fractional order COVID-19 model with a case study of Saudi Arabia, *Results Phys.*, **21** (2021), 103787. https://doi.org/10.1016/j.rinp.2020.103787

20. Y. M. Chu, M. F. Yassen, I. Ahmad, P. Sunthrayuth, M. A. Khan, A fractional SARS-CoV-2 model with Atangana-Baleanu derivative: application to fourth wave, *Fractals*, **30** (2022), 2240210. https://doi.org/10.1142/S0218348X22402101

21. P. Pandey, Y. M. Chu, J. F. Gmez-Aguilar, H. Jahanshahi, A. A. Aly, A novel fractional mathematical model of COVID-19 epidemic considering quarantine and latent time, *Results Phys.*, **26** (2021), 104286. https://doi.org/10.1016/j.rinp.2021.104286

22. A. Omame, H. Rwezaura, M. L. Diagne, COVID-19 and dengue co-infection in Brazil: optimal control and cost-effectiveness analysis, *Eur. Phys. J. Plus*, **136** (2021), 1090. https://doi.org/10.1140/epjp/s13360-021-02030-6

23. A. Omame, M. E. Isah, M. Abbas, A fractional order model for dual variants of COVID-19 and HIV co-infection via Atangana-Baleanu derivative, *Alex. Eng. J.*, **61** (2022), 9715–9731. https://doi.org/10.1016/j.aej.2022.03.013

24. N. Ringa, M. L. Diagne, H. Rwezaura, A. Omame, S. Y. Tchoumi, J. M. Tchuenche, HIV and COVID-19 co-infection: a mathematical model and optimal control, *Inf. Med. Unlocked*, **31** (2022), 100978. https://doi.org/10.1016/j.imu.2022.100978

25. I. M. Hezam, A. Foul, A. Alrasheedi, A dynamic optimal control model for COVID-19 and cholera co-infection in Yemen, *Adv. Differ. Equations*, **2021** (2021), 108. https://doi.org/10.1186/s13662-021-03271-6

26. W. Y. Shen, Y. M. Chu, M. ur Rahman, I. Mahariq, A. Zeb, Mathematical analysis of HBV and HCV co-infection model under nonsingular fractional order derivative, *Results Phys.*, **28** (2021), 104582. https://doi.org/10.1016/j.rinp.2021.104582

27. M. Majumder, P. K. Tiwari, S. Pal, Impact of saturated treatments on HIV-TB dual epidemic as a consequence of COVID-19: optimal control with awareness and treatment, *Nonlinear Dyn.*, **109** (2022), 143–176. https://doi.org/10.1007/s11071-022-07395-6

28. J. M. Mutua, F. B. Wang, N. K. Vaidya, Modeling malaria and typhoid fever co-infection dynamics, *Math. Biosci.*, **264** (2015), 128–144. https://doi.org/10.1016/j.mbs.2015.03.014

29. A. Omame, M. Abbas, C. P. Onyenegecha, A fractional-order model for COVID-19 and tuberculosis co-infection using Atangana-Baleanu derivative, *Chaos Solitons Fract.*, **153** (2021), 111486. https://doi.org/10.1016/j.chaos.2021.111486

30. A. Omame, M. Abbas, C. P. Onyenegecha, A fractional order model for the co-interaction of COVID-19 and hepatitis B virus, *Results Phys.*, **37** (2022), 105498. https://doi.org/10.1016/j.rinp.2022.105498

31. B. E. Bassey, J. U. Atsu, Global stability analysis of the role of multi-therapies and non-pharmaceutical treatment protocols for COVID-19 pandemic, *Chaos Solitons Fract.*, **143** (2021), 110574. https://doi.org/10.1016/j.chaos.2020.110574

32. A. S. Bhadauria, R. Pathak, M. Chaudhary, A SIQ mathematical model on COVID-19 investigating the lockdown effect, *Infect. Dis. Modell.*, **6** (2021), 244–257. https://doi.org/10.1016/j.idm.2020.12.010

33. J. Couras, I. Area, J. J. Nieto, C. J. Silva, D. F. M. Torres, Optimal control of vaccination and plasma transfusion with potential usefulness for COVID-19, In: P. Agarwal, J. J. Nieto, M. Ruzhansky, D. F. M. Torres, *Analysis of infectious disease problems (COVID-19) and their global impact*, Springer, 2021. https://doi.org/10.1007/978-981-16-2450-6_23

34. P. Wintachai, K. Prathom, Stability analysis of SEIR model related to efficiency of vaccines for COVID-19 situation, *Heliyon*, **7** (2021), e06812. https://doi.org/10.1016/j.heliyon.2021.e06812

35. S. Berkane, I. Harizi, A. Tayebi, Modeling the effect of population-wide vaccination on the evolution of COVID-19 epidemic in Canada, *medRxiv*, 2021. https://doi.org/10.1101/2021.02.05.21250572

36. M. A. Acuña-Zegarra, S. Díaz-Infante, D. Baca-Carrasco, D. Olmos-Liceaga, COVID-19 optimal vaccination policies: a modeling study on efficacy, natural and vaccine-induced immunity responses, *Math. Biosci.*, **337** (2021), 108614. https://doi.org/10.1016/j.mbs.2021.108614

37. B. Buonomo, R. D. Marca, A. d'Onofrio, M. Groppi, A behavioural modelling approach to assess the impact of COVID-19 vaccine hesitancy, *J. Theor. Biol.*, **534** (2022), 110973. https://doi.org/10.1016/j.jtbi.2021.110973

38. A. Fridman, R. Gershon, A. Gneezy, COVID-19 and vaccine hesitancy: a longitudinal study, *Plos One*, **16** (2021), e0250123. https://doi.org/10.1371/journal.pone.0250123

39. N. Gul, R. Bilal, E. A. Algehyne, The dynamics of fractional order Hepatitis B virus model with asymptomatic carriers, *Alex. Eng. J.*, **60** (2021), 3945–3955. https://doi.org/10.1016/j.aej.2021.02.057

40. F. B. Agusto, Optimal isolation control strategies and cost-effectiveness analysis of a two-strain avian influenza model, *Biosystems*, **113** (2013), 155–164. https://doi.org/10.1016/j.biosystems.2013.06.004

41. P. van den Driessche, J. Watmough, Reproduction numbers and sub-threshold endemic equilibria for compartmental models of disease transmission, *Math. Biosci.*, **180** (2002), 29–48. https://doi.org/10.1016/S0025-5564(02)00108-6

42. J. P. L. Salle, *The stability of dynamical systems*, SIAM, 1976.

43. L. Xue, H. Y. Zhang, W. Sun, C. Scoglio, Transmission dynamics of multi-strain dengue virus with cross-immunity, *Appl. Math. Comput.*, **392** (2021), 125742. https://doi.org/10.1016/j.amc.2020.125742

44. L. Pontryagin, V. Boltyanskii, R. Gamkrelidze, E. Mishchenko, *The mathematical theory of optimal control process*, 4 Eds., Routledge, 1962.

AIMS Press